9. Yu, G. & Heeger, A. J. High efficiency photonic devices made with semiconducting polymers. *Synth. Met.* **85,** 1183–1186 (1987).
10. Friend, R. H. *et al.* Electronic excitations in luminescent conjugated polymers. *Solid State Commun.* **102,** 249–258 (1997).
11. Tada, K., Onoda, M., Zakhidov, A. A. & Yoshino, K. Characteristics of poly(p-pyridyl vinylene)/poly(3-alkylthiophene) heterojunction photocell. *Jpn. J. Appl. Phys. Pt2-Lett.* **36,** L306–L309 (1997).
12. Takahashi, K. *et al.* Enhanced quantum yield in porphyrin/electron-donor double-layer solar cells. *Solar Energy Mater. Solar Cells* **45,** 127–139 (1997).
13. Yoshino, K., Tada, K., Fujii, A., Conwell, E. M. & Zakhidov, A. A. Novel photovoltaic devices based on donor-acceptor molecular and conducting polymer systems. *IEEE Trans. Electron. Devices* **44,** 1315–1324 (1997).
14. Roman, L. S., Andersson, M. R., Yohannes, T. & Inganäs, O. Photodiode performance and nanostructure of poly(thiophene)/C_{60} blends. *Adv. Mater.* **9,** 1164–1168 (1997).
15. Yang, C. Y. & Heeger, A. J. Morphology of composites of semiconducting polymers mixed with C_{60}. *Synth. Met.* **83,** 85–88 (1996).
16. Moratti, S. C. *et al.* High electron-affinity polymers for LEDs. *Synth. Met.* **71,** 2117–2120 (1995).
17. Greenham, N. C., Moratti, S. C., Bradley, D. D. C., Friend, R. H. & Holmes, A. B. Efficient polymer-based light-emitting diodes based on polymers with high electron affinities. *Nature* **365,** 628–630 (1993).
18. Baigent, D. R. *et al.* Light-emitting diodes fabricated with conjugated polymers—recent progress. *Synth. Met.* **67,** 3–10 (1994).
19. Andersson, M. R. *et al.* Electroluminescence from substituted poly(thiophenes)—from blue to near-infrared. *Macromolecules* **28,** 7525–7529 (1995).
20. Berggren, M. *et al.* Thermal control of near-infrared and visible electroluminescence in alkyl-phenyl substituted polythiophenes. *Appl. Phys. Lett.* **65,** 1489–1491 (1994).
21. Andersson, M. R. *et al.* Regioselective polymerization of 3-(4-octylphenyl)thiophene with $FeCl_3$. *Macromolecules* **27,** 6503–6506 (1994).
22. de Mello, J. C., Wittmann, H. F. & Friend, R. H. An improved experimental determination of external photoluminescence quantum efficiency. *Adv. Mater.* **9,** 230–232 (1997).
23. Granström, M. *et al.* Self-organizing polymer films—a route to novel electronic devices based on conjugated polymers. *Supramol. Sci.* **4,** 27–34 (1997).
24. O'Regan, B. & Grätzel, M. A low-cost, high-efficiency solar cell based on dye-sensitized colloidal TiO_2 films. *Nature* **353,** 737–740 (1991).

Acknowledgements. Financial support from the Engineering and Physical Sciences Research Council, the European Commission (TMR Marie Curie fellowship and TMR Network SELOA), and from CNPq, Brazilian government, is gratefully acknowledged.

Correspondence and requests for materials should be addressed to R.H.F. (e-mail: rhf10@cam.ac.uk).

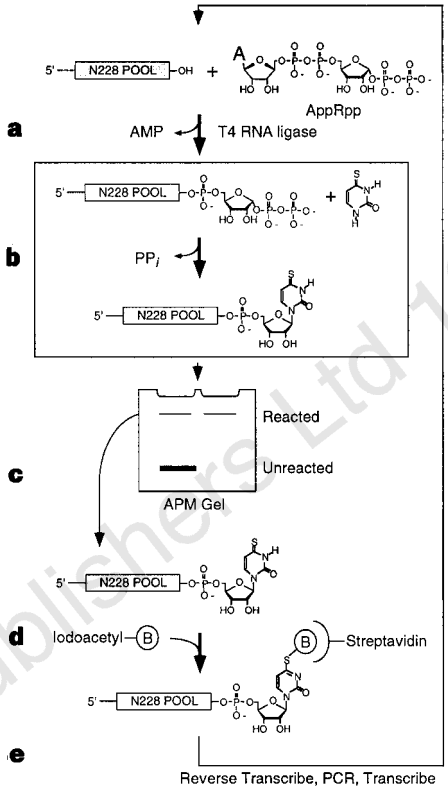

Figure 2 *In vitro* selection scheme. Symbols: PP_i, pyrophosphate; B, biotin. **a**, Tethering pool RNA to pRpp by using T4 RNA ligase and adenylylated pRpp (AppRpp). **b**, ^{4S}U synthesis promoted by active sequences within the initial pool. **c**, Enrichment of reacted sequences by using APM gels. One lane (left) contained radiolabelled pool RNA. The other lane (right) contained radiolabelled synthetic standard to mark the location of the reacted RNA. After the first round of selection, catalysts were enriched by serial purification on two APM gels. **d**, Further enrichment of ^{4S}U-containing sequences by derivation with iodoacetyl-LC-biotin (Pierce) and capture with streptavidin magnetic beads. **e**, Amplification of enriched RNA by reverse transcription, PCR and transcription. The amplified RNA was then subjected to another round of selection *in vitro*.

RNA-catalysed nucleotide synthesis

Peter J. Unrau & David P. Bartel

Whitehead Institute for Biomedical Research, and Department of Biology, MIT, 9 Cambridge Center, Cambridge, Massachusetts 02142, USA

The 'RNA world' hypothesis proposes that early life developed by making use of RNA molecules, rather than proteins, to catalyse the synthesis of important biological molecules[1]. It is thought, however, that the nucleotides constituting RNA were scarce on early Earth[1–4]. RNA-based life must therefore have acquired the ability to synthesize RNA nucleotides from simpler and more readily available precursors, such as sugars and bases. Plausible prebiotic synthesis routes have been proposed for sugars[5], sugar phosphates[6] and the four RNA bases[7–11], but the coupling of these molecules into nucleotides, specifically pyrimidine nucleotides, poses a challenge to the RNA world hypothesis[1–3]. Here we report the application of *in vitro* selection to isolate RNA molecules that catalyse the synthesis of a pyrimidine nucleotide at their 3′ terminus. The finding that RNA can catalyse this type of reaction, which is modelled after pyrimidine synthesis in contemporary metabolism, supports the idea of an RNA world that included nucleotide synthesis and other metabolic pathways mediated by ribozymes.

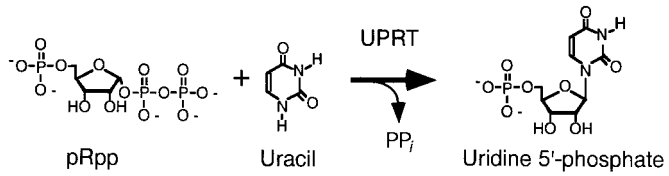

Figure 1 UPRT-catalysed synthesis of uridine 5′-phosphate from pRpp and uracil.

In modern metabolism, pyrimidine nucleotides are synthesized from activated ribose (pRpp) and pyrimidine bases (such as uracil or orotate). For example, uracil phosphoribosyltransferase (UPRT) catalyses the reaction shown in Fig. 1. The chemistry of this reaction, nucleophilic attack on carbon after release of pyrophosphate, is central to the biosynthesis of nucleotides and amino acids (histidine and tryptophan), yet absent from known ribozyme reactions. The reaction differs from known RNA-catalysed reactions in other key respects: it occurs by an S_N1 mechanism (involving the stabilization of an oxocarbocation at the reaction centre, C1′ of ribose)[12,13], and uracil is significantly smaller than the smallest ribozyme substrates.

To explore the ability of RNA to promote nucleotide synthesis, we performed an iterative selection *in vitro* to isolate from random sequences ribozymes that synthesized a pyrimidine nucleotide at their 3′ terminus (Fig. 2). The initial pool of sequences contained $> 1.5 \times 10^{15}$ different RNA molecules, each with 228 random positions. To begin each selective round, pRpp was attached to the 3′ end of pool RNA. RNA-pRpp conjugates were incubated with a uracil analogue, 4-thiouracil (^{4S}Ura), to allow those sequences capable of glycosidic bond formation the opportunity to link their tethered ribose to ^{4S}Ura. RNAs attached to the newly synthesized nucleotide, 4-thiouridine (^{4S}U), were then enriched, amplified, and subjected to another round of selection–amplification. ^{4S}U was chosen as the desired product because the thione at position 4

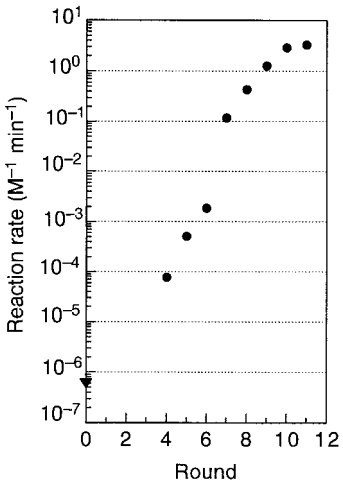

Figure 3 Increased ribozyme activity with successive rounds of selection. The upper bound for the uncatalysed rate is also plotted (triangle). Rounds 4 to 6 included error-prone PCR amplification, as described[17]. From rounds 7 to 10 the stringency of the selection was increased exponentially by decreasing both ^{4S}Ura concentration (from 8 mM to 40 μM) and incubation time (from 18 h to 7.5 min). Reaction rates were calculated by dividing the observed initial rate by the ^{4S}Ura incubation concentration.

interacts strongly with a number of thiophilic reagents[14], facilitating the efficient enrichment of RNAs with a single ^{4S}U nucleotide. In other respects, sulphur substitution of the 4-keto oxygen of uracil has little effect; tautomeric patterns of the N_1 and N_3 protons are comparable, whereas the sulphur substitution lowers the pK_a of uracil by less than one unit to 8.4 (refs 15, 16). After four rounds of selection–amplification, ribozyme activity was readily detected (Fig. 3). Pool activity increased another 50,000-fold in response to seven additional selective rounds that included shorter incubation times, lower ^{4S}Ura concentration and mutagenic amplification (Fig. 3).

Ribozymes that had undergone 11 rounds of selection were cloned, and 35 random clones were sequenced. A family of 25 related sequences generated by the mutation of a single ancestral sequence dominated the round-11 isolates and was designated family A (Fig. 4a). The remaining isolates represented two other families, family B (eight isolates) and family C (two isolates). Restriction analysis of PCR DNA from each round of selection[17] indicated that these were the only three families of nucleotide-synthesizing ribozymes to emerge to detectable levels (≥4% of the population) during the entire course of the selection and evolution (data not shown).

Synthesis of authentic tethered ^{4S}U was confirmed for representatives of each ribozyme family by nearest-neighbour analysis of end-labelled product (Fig. 5). The ribozyme-synthesized nucleotide precisely comigrated with the 4-thiouridine 3′-phosphate (^{4S}Up) standard in all six separation systems tested: two polyacrylamide gel systems and four thin-layer chromatography (TLC) systems. An analysis utilizing a two-dimensional TLC system known to resolve the many different modified bases of ribosomal RNA[18] is shown (Fig. 5).

Isolates from each family promoted nucleotide formation with apparent second-order rate constants (k_{cat}/K_m values) up to 10^7 times greater than our upper bound on the uncatalysed reaction rate (Fig. 4). In attempts to detect the uncatalysed reactions, a radiolabelled pRpp-derivatized oligonucleotide was incubated with ^{4S}Ura and the reaction mixture was resolved on APM gels. ^{4S}U synthesis was not detected, even though these assays would have readily detected a reaction as slow as 6×10^{-7} M^{-1} min^{-1}. The rates of a family A isolate fit well to a Michaelis–Menten curve with an apparent K_m of 28 ± 4 mM and a k_{cat} of 0.13 ± 0.012 min^{-1} (means ± s.e.m.; Fig. 4b), although it should be noted that solubility constraints prevented rate measurements with ^{4S}Ura concentrations above 14 mM. Representatives from the other two sequence families had comparable k_{cat}/K_m values but did not begin to display saturable behaviour at soluble concentrations of ^{4S}Ura (Fig. 4b), suggesting poorer binding to ^{4S}Ura but faster catalysis on encountering ^{4S}Ura.

All three ribozymes had high specificity for the ^{4S}Ura substrate. No thio-containing product was detected on APM gels after body-labelled ribozyme-pRpp was incubated with any of six other thio-substituted pyrimidine bases (2-thiouracil, 2,4-thiouracil, 2-thiocytosine, 2-thiopyrimidine, 2-thiopyridine and 5-carboxy-2-thiouracil; limits of detection, 4×10^{-3} to 1×10^{-4} M^{-1} min^{-1}, depending on whether the product migrated to an area of the gel with high or low background). The family A isolate reacted very slowly with radiolabelled uracil, with a rate (2×10^{-4} M^{-1} min^{-1}) comparable to that of the pool with ^{4S}Ura after four rounds of selection.

Protein enzymes that synthesize pyrimidine nucleotides are thought to catalyse an S_N1 reaction by stabilizing an oxocarbocation at the C1′ carbon of the reaction centre[12,13]. One challenge for these enzymes is to avoid the hydrolysis of pRpp to ribose 5′-phosphate and pyrophosphate, which occurs if water rather than the pyrimidine base is proximal to the highly reactive carbocation. The enzyme that synthesizes orotidine (6-carboxyuridine) avoids hydrolysing pRpp by excluding water from the active site and by promoting carbocation formation only after a conformational change induced by binding of orotate (6-carboxyuracil)[12,13]. As with the metabolic enzymes, our ribozymes were selected to avoid pRpp hydrolysis; any catalyst that hydrolysed its pRpp moiety before ^{4S}Ura addition (for example, during the T4 RNA ligase incubation needed to attach the pRpp) would have been inactive for ^{4S}U synthesis. Thus, we examined the degree to which the ribozymes promoted the hydrolysis of the tethered pRpp. Ribozymes from the three families promoted the hydrolysis of their pRpp moiety at rates 12–23 times faster than uncatalysed hydrolysis (Fig. 4a). Nevertheless their k_{cat} values for ^{4S}U formation were ≥60 times faster than their rates of catalysed hydrolysis. Either RNA does have the ability to exploit highly reactive reaction intermediates or these ribozymes have employed a new strategy for promoting glycosidic bond formation, that is, by stabilizing a transition state with more S_N2 character.

As with many ribozymes and the metabolic enzymes that synthesize nucleotides, all three ribozyme families required divalent cations for activity. For each round of selection, Mg^{2+} (25 mM), Ca^{2+} (1 mM) and Mn^{2+} (0.5 mM) had been provided. However, Ca^{2+} was dispensable for all three families. Although the three families were active in the presence of Mn^{2+} as the only divalent cation, all preferred Mg^{2+} over Mn^{2+} as the major divalent cation. The family A isolate did not require Mn^{2+}, with only a twofold decrease in activity observed in the absence of Mn^{2+}. The family B and C ribozymes required Mn^{2+}, with the activity in the presence of 25 mM Mg^{2+} reaching a plateau at 1 mM Mn^{2+}. The family B ribozyme did not require Mn^{2+} for stimulating pRpp hydrolysis, suggesting that for this family Mn^{2+} has a role in the binding or proper orientation of the ^{4S}Ura, consistent with the thiophilic nature of Mn^{2+} compared with Mg^{2+} and Ca^{2+} (ref. 19).

Ribozymes of an RNA world would have needed to promote numerous reactions involving small organic molecules[20]. An important question in this regard is whether RNA can perform covalent chemistry with substrates smaller than purine nucleosides. Ribonucleosides as small as adenosine and 2-aminopurine (M_r 267.2) are substrates for self-splicing intron derivatives[21,22]. ^{4S}Ura (M_r 128.1) is half the size of these nucleoside substrates and within the size range of the smallest aptamer targets, valine and arginine[23] (M_r 117.2 and 174.2, respectively). The findings that a catalytic RNA

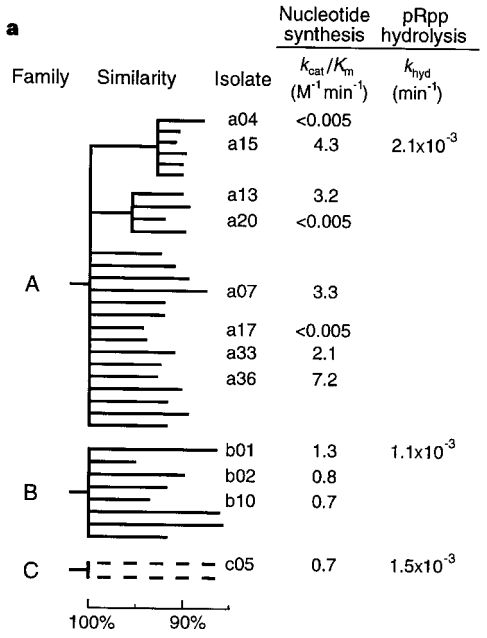

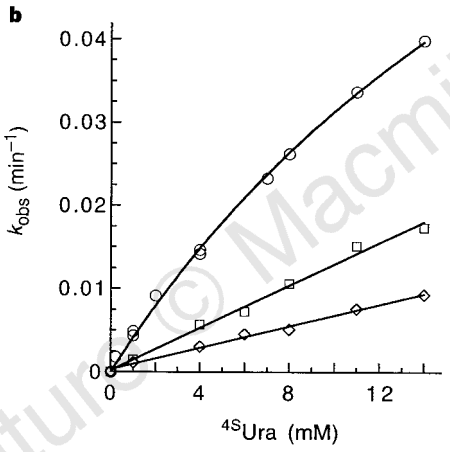

Figure 4 Analysis of ribozyme sequences and their catalytic proficiencies. **a**, Three families of ribozymes with rates of ^{4S}U production and pRpp hydrolysis. Sequence analysis is summarized by family trees, with each branch terminus representing one of the 35 sequenced isolates. Similarity to the family consensus sequence varied from 94 to 86%, as indicated by the horizontal length of the branches. Family A has two dominant subfamilies, which presumably emerged through preferential expansion of superior early lineages. Because the family C consensus sequence could not be fully determined from only two isolates, similarity to the consensus is reported as a range (dashed lines). **b**, Rate of nucleotide formation (k_{obs}) as a function of ^{4S}Ura concentration for isolates a15 (circles), b01 (squares) and c05 (diamonds). The rates of isolates b01 and c05 fit well to linear functions indicating k_{cat}/K_m values of 1.29 ± 0.03 and $0.67 \pm 0.02\,M^{-1}\,min^{-1}$, respectively. The line shown for isolate a15 is the non-linear least-squares fit of a Michaelis–Menten curve to the data and suggests an apparent K_m of 28 ± 4 mM and a k_{cat} of $0.13 \pm 0.012\,min^{-1}$ (mean ± s.e.m.), although these values must be viewed with caution because solubility constraints prevented the examination of ^{4S}Ura concentrations above 14 mM. For example, we cannot discount the possibility that ^{4S}Ura was beginning to occupy an inhibitory site rather than the catalytic site. The linear behaviour of the other two isolates suggests that ^{4S}Ura within this concentration range does not aggregate or affect metal-ion availability.

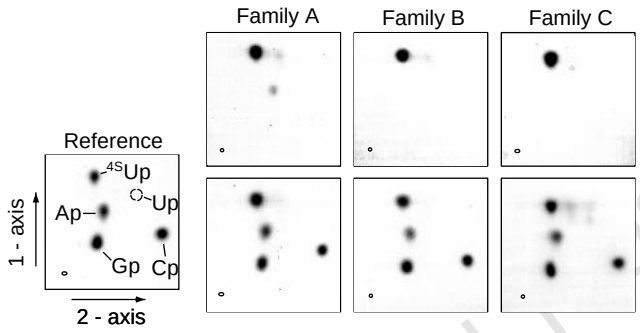

Figure 5 Two-dimensional TLC analysis[18] of ribozyme-synthesized ^{4S}U after labelling and digestion with nuclease. Ribozyme product RNA was extended by one nucleotide by using α-^{32}P-cordycepin triphosphate (3′-deoxyATP) and poly(A) polymerase, then purified on an APM gel. Ribonuclease T2 digestion reduced all the labelled material into nucleoside 3′-phosphates, with the labelled phosphate residing on the ribozyme-synthesized nucleotide. Digests were spotted on 10 × 10 cm cellulose TLC plates (Baker flex) presoaked in 1:10 saturated-$(NH_4)_2SO_4$:H_2O. The first axis was run in 80% v/v ethanol, and after air-drying for 5 min, the second axis of 40:1 saturated-$(NH_4)_2SO_4$:isopropanol was run. The reference panel shows the migration of ^{4S}Up, Up, Ap, Cp and Gp. Unlabelled or body-labelled ^{4S}U-containing RNA was included as carrier in the digestion (top and bottom panels, respectively). Carrier RNA was generated by transcription, with ^{4S}UTP replacing UTP.

can specifically recognize and utilize such a substrate and that RNA can efficiently promote the chemistry of glycosidic bond formation support the prospects of ribozyme-based metabolic pathways in the RNA world. Another important step would be to generate catalytic sequences capable of using not one but two small-molecule substrates. With regard to this goal it is encouraging that after optimization by evolution and engineering *in vitro*, a ribozyme motif initially selected on the basis of a reaction using an attached nucleoside triphosphate was able to promote a reaction using free nucleoside triphosphates[24]. Similarly, our new ribozymes offer a basis for developing catalysts that synthesize ^{4S}U from two small molecules, ^{4S}Ura and pRpp. □

Methods

Pool construction and amplification. The double-stranded DNA pool with sequence *TTCTAATACGACTCACTATA*GGACCGAGAAGTTACCC-N_{76}-CCTTGG-N_{76}-GGCACC-N_{76}-ACGCACATCGCAGCAAC (italics, T7 promoter; -N_{76}-, 76-nucleotide random-sequence segment) was constructed starting with three synthetic single-stranded pools, as described previously[17,25]. The phosphoramidite ratio for random-sequence DNA synthesis was normalized to account for differing coupling rates (0.26:0.25:0.29:0.20 dA:dC:dG:dT molar ratio). Sequencing 2,030 random-sequence positions from arbitrary clones verified that the nucleotide composition was nearly equal (529:519:482:500 A:C:G:T). The DNA pool was transcribed *in vitro* and 16.4 nmol RNA (six copies, on average, of each pool sequence) were used for the first round of selection.

Tethering pRpp and p^{4S}U to RNA. pRpp was linked to RNA by exploiting the finding that specificity for the donor substrate of T4 RNA ligase can be bypassed by pre-adenylylation[26] (Fig. 2a). Adenylylated pRpp (AppRpp) was synthesized by reacting 300 mM adenosine 5′-phosphorimidazolide[27] with 600 mM pRpp in 200 mM $MgCl_2$ for 2 h at 50 °C. After ligation (2–4 μM gel-purified RNA, 65 μM HPLC-purified AppRpp, 50 mM HEPES pH 8.3, 10 mM $MgCl_2$, 3.3 mM dithiothreitol (DTT), 10 μg/ml BSA, 8.3% v/v glycerol, 1 U μl^{-1} enzyme from Pharmacia, for 4 h at room temperature) and extraction with phenol–chloroform, RNA was recovered by precipitation with ethanol. The efficacy of ligation was verified by using matrix-assisted mass spectrometry of a 9-nt ligation product before and after treatment with alkaline phosphatase, which removed the 1′ pyrosphosphate. At each round, the efficiency of ligation

to the pool RNA was determined by the gel mobility of 3′-terminal fragments cleaved by a DNA enzyme[28] targeted to the 3′ constant segment. RNAs extended with ^{4S}U (for use as synthetic standards) were generated, using App^{4S}U instead of AppRpp.

Ribozyme selection. ^{4S}Ura was synthesized[29] and further purified by reverse-phase HPLC. For each round of selection the RNA-pRpp pool was incubated with ^{4S}Ura (Fig. 2b) using the concentrations and incubation times outlined in Fig. 3 (≤0.3 μM pool RNA, 50 mM Tris-HCl pH 7.5, 150 mM KCl, 25 mM $MgCl_2$, 1 mM $CaCl_2$, 0.5 mM $MnCl_2$ at 23 °C). Ribozyme reactions were stopped by the addition of one volume of gel loading buffer (90% formamide, 50 mM EDTA). RNA with a 3′-terminal ^{4S}U was resolved from other species on denaturing APM gels[14,30] (8 M urea/5% polyacrylamide gels, cast with 80 μM *N*-acryloylaminophenylmercuric acetate). During each round of selection, the ribozyme reaction was split in half. One half contained radiolabelled pool RNA that facilitated the detection and purification of emergent ribozymes; the other half contained unlabelled pool and a trace amount of radiolabelled synthetic standard (an RNA pool with a 3′-terminal ^{4S}U but with primer-binding sequences incompatible with reverse transcription and PCR) that was used to locate and monitor the recovery of reacted RNA. The gel fragment containing RNA-^{4S}U was excised (Fig. 2c), and RNA was eluted in 300 mM NaCl, 20 mM DTT, then precipitated with ethanol. After round 1, RNA containing ^{4S}U was further purified on a second mercury gel and then biotinylated (Fig. 2d) by resuspending precipitated RNA in 25 mM potassium phosphate pH 8.4, 3 mM iodoacetyl-LC-biotin (Pierce), 50% v/v dimethylformamide. After 3 h at room temperature in the dark, the reaction was quenched with DTT and diluted 10-fold; RNA was then twice precipitated with ethanol to remove excess biotin. About 75% of material end-labelled with ^{4S}U was biotinylated, as judged by a streptavidin gel-shift assay. Capture of biotinylated RNA, reverse transcription, PCR amplification and transcription *in vitro* were as described previously[25].

Ribozyme assays. Unless stated otherwise, ribozyme isolates were assayed under conditions similar to those of the selection (0.5 μM ^{32}P-labelled ribozyme RNA, 50 mM *N*,*N*-(bis-2-hydroxyethyl)-2-aminoethanesulphonic acid (BES) pH 7.5, 150 mM KCl, 25 mM $MgCl_2$, 0.5 mM $MnCl_2$ at 23 °C). The rate of ^{4S}U synthesis (k_{obs}) at a given ^{4S}Ura concentration was determined by the best fit of k and β to the equation $F = \beta(1 - e^{-kt})$, where F is the fraction reacted (ascertained by phosphorimaging of the APM gel), $k = k_{obs} + k_{hyd}$, $\beta = F_{max}k_{obs}/(k_{obs} + k_{hyd})$, k_{hyd} is the rate of pRpp hydrolysis, and t is time. F_{max}, the maximal active fraction (typically 0.15–0.20) was determined by using time courses with ^{4S}Ura in excess of 4 mM. Factors contributing to the low F_{max} values included: incomplete pRpp ligation (lowering F_{max} by 10–30%), 3′ heterogeneity from untemplated residues added during transcription (lowering F_{max} by 40–50%), and ribozyme misfolding. The k_{hyd} values were determined by varying ^{4S}Ura concentration and observing differences in the asymptotic fraction reacted. The k_{hyd} values were confirmed independently by monitoring the inactivation of RNA-pRpp in the absence of ^{4S}Ura. The rate of uridine synthesis was determined by using isolate a15 and a random-sequence control RNA, both activated with pRpp. Each RNA (7 μM) was incubated with 0.5 mCi [5,6-^{3}H]uracil (NEN) in standard buffer conditions. At 0, 2, 4 and 8 h, 160 μl aliquots were quenched by the addition of EDTA and unlabelled uracil. RNA was filtered (Centricon spin filters; Amicon), purified on a polyacrylamide gel and precipitated with ethanol. Uracil counts associated with the RNA were determined by scintillation (Formula-989 fluid, Packard) and corrected for RNA recovery. A similar approach with [2-^{14}C]uracil indicated a comparable rate (within twofold). Additional analysis of RNA recovered from the scintillation fluid (precipitation with NaCl and six volumes of ethanol, and resuspension with unlabelled uridine) confirmed that the incorporated counts were from 3′-terminal uridine synthesis; RNA was base-hydrolysed and nucleotides were separated by reverse-phase HPLC and scintillation-counted. The uncatalysed reaction rates were examined with a 9-nt RNA-pRpp conjugate that was ^{32}P-labelled at its 5′ terminus. After incubation with 6.4 mM ^{4S}Ura for 4 days in the buffer used for the selection, no RNA-p^{4S}U product was observed on APM gels. A single gel would have readily detected uncatalysed RNA-p^{4S}U formation with a rate $\geq 2 \times 10^{-6}$ M^{-1} min^{-1} (correcting for the RNA-pRpp lost to hydrolysis), whereas a serial APM gel analysis lowered detection limits to 6×10^{-7} M^{-1} min^{-1}. The RNA-pRpp hydrolysed during the 4-day time course indicated an uncatalysed k_{hyd} of 9×10^{-5} min^{-1}.

Received 13 March; accepted 20 July 1998.

1. Joyce, G. F. & Orgel, L. E. in *The RNA World* (eds Gesteland, R. F. & Atkins, J. F.) 1–25 (Cold Spring Harbor Lab., Cold Spring Harbor, NY, 1993).
2. Fuller, W. D., Sanchez, R. A. & Orgel, L. E. Studies in prebiotic synthesis VI. Synthesis of purine nucleosides. *J. Mol. Biol.* **67,** 25–33 (1972).
3. Fuller, W. D., Sanchez, R. A. & Orgel, L. E. Studies in prebiotic synthesis VII. Solid-state synthesis of purine nucleosides. *J. Mol. Evol.* **1,** 249–257 (1972).
4. Larralde, R., Robertson, M. P. & Miller, S. L. Rates of decomposition of ribose and other sugars: implications for chemical evoution. *Proc. Natl Acad. Sci. USA* **92,** 8158–8160 (1995).
5. Mizuno, T. & Weiss, A. H. Synthesis and utilization of formose sugars. *Adv. Carbohyd. Chem. Biochem.* **29,** 173–227 (1974).
6. Pitsch, S., Eschenmoser, A., Gedulin, B., Hui, S. & Arrhenius, G. Mineral induced formation of sugar phosphates. *Origin Life Evol. Biosphere* **25,** 297–334 (1995).
7. Oro, J. Mechanism of synthesis of adenine from hdyrogen cyanide under possible primitive earth conditions. *Nature* **191,** 1193–1194 (1961).
8. Sanchez, R. A., Ferris, J. P. & Orgel, L. E. Studies in prebiotic synthesis. II. Synthesis of purine precursors and amino acids from aqueous hydrogen cyanide. *J. Mol. Biol.* **30,** 223–253 (1967).
9. Ferris, J. P., Sanchez, R. A. & Orgel, L. E. Studies in prebiotic synthesis. 3. Synthesis of pyrimidines from cyanoacetylene and cyanate. *J. Mol. Biol.* **33,** 693–704 (1968).
10. Stoks, P. G. & Schwartz, A. W. Uracil in carbonaceous meteorites. *Nature* **282,** 709–710 (1979).
11. Robertson, M. P. & Miller, S. L. An efficient prebiotic synthesis of cytosine and uracil. *Nature* **375,** 772–774 (1995).
12. Bhatia, M. B., Vinitsky, A. & Grubmeyer, C. Kinetic mechanism of orotate phosphoribosyltransferase from *Salmonella typhimurium*. *Biochemistry* **29,** 10480–10487 (1990).
13. Tao, W., Grubmeyer, C. & Blanchard, J. S. Transition state structure of *Salmonella typhimurium* orotate phosphoribosyltransferase. *Biochemistry* **35,** 14–21 (1996).
14. Igloi, G. L. Interaction of tRNAs and of phosphorothioate-substituted nucleic acids with an organomercurial. Probing the chemical environment of thiolated residues by affinity electrophoresis. *Biochemistry* **27,** 3842–3849 (1988).
15. Wierzchowski, K. L., Litonska, E. & Shugar, D. Infrared and ultraviolet studies on the tautomeric equilibria in aqueous medium between monoanionic species of uracil, thymine, 5-fluorouracil, and other 2,4-diketopyrimidines. *J. Am. Chem. Soc.* **87,** 4621–4629 (1965).
16. Psoda, A., Kazimierczuk, Z. & Shugar, D. Structure and tautomerism of the neutral and monoanionic forms of 4-thiouracil derivatives. *J. Am. Chem. Soc.* **96,** 6832–6839 (1974).
17. Bartel, D. P. & Szostak, J. W. Isolation of new ribozymes from a large pool of random sequences. *Science* **261,** 1411–1418 (1993).
18. Gray, M. W. The presence of 2′-O-methylpseudouridine in the 18S + 26S ribosomal ribonucleates of wheat embryo. *Biochemistry* **13,** 5453–5463 (1974).
19. Jaffe, E. K. & Cohn, M. Diastereomers of the nucleoside phosphorothioates as probes of the structure of the metal nucleotide substrates and of the nucleotide binding site of yeast hexokinase. *J. Biol. Chem.* **254,** 10839–10845 (1979).
20. Benner, S. A., Ellington, A. D. & Tauer, A. Modern metabolism as a palimpsest of the RNA world. *Proc. Natl Acad. Sci. USA* **86,** 7054–7058 (1989).
21. Michel, F., Hanna, M., Green, R., Bartel, D. P. & Szostak, J. W. The guanosine binding site of the *Tetrahymena* ribozyme. *Nature* **342,** 391–395 (1989).
22. Been, M. D. & Perrotta, A. T. Group I intron self-splicing with adenosine: evidence for a single nucleoside-binding site. *Science* **252,** 434–437 (1991).
23. Gold, L., Polisky, B., Uhlenbeck, O. & Yarus, M. Diversity of oligonucleotide functions. *Annu. Rev. Biochem.* **64,** 763–797 (1995).
24. Ekland, E. H. & Bartel, D. P. RNA-catalysed RNA polymerization using nucleoside triphosphates. *Nature* **382,** 373–376 (1996).
25. Ekland, E. H. & Bartel, D. P. The secondary structure and sequence optimization of an RNA ligase ribozyme. *Nucleic Acids Res.* **23,** 3231–3238 (1995).
26. England, T. E., Gumport, R. I. & Uhlenbeck, O. C. Dinucleoside pyrophosphates are substrates for T4-induced RNA ligase. *Proc. Natl Acad. Sci. USA* **74,** 4839–4842 (1977).
27. Lohrmann, R. & Orgel, L. E. Preferential formation of (2′-5′)-linked internucleotide bonds in non-enzymatic reactions. *Tetrahedron* **34,** 853–855 (1978).
28. Santoro, S. W. & Joyce, G. F. A general purpose RNA-cleaving DNA enzyme. *Proc. Natl Acad. Sci. USA* **94,** 4262–4266 (1997).
29. Mizuno, Y., Ikehara, M. & Watanabe, K. A. Potential antimetabolites. I. Selective thiation of uracil and 1,2,4-triazine-3,5(2*H*,4*H*)-dione (6-azauracil). *Chem. Pharmac. Bull.* **10,** 647–652 (1962).
30. Wecker, M., Smith, D. & Gold, L. *In vitro* selection of a novel catalytic RNA: characterization of a sulfur alkylation reaction and interaction with a small peptide. *RNA* **2,** 982–994 (1996).

Acknowledgements. We thank J. Stubbe, P. Zamore and members of the lab for helpful comments on the manuscript, and G. Joyce for providing the sequence of the RNA-cleaving DNA enzyme[28] before publication. This work was supported by an MRC (Canada) postdoctoral fellowship to P.J.U. and a grant from the Searle Scholars Program/The Chicago Community Trust to D.P.B.

Correspondence and requests for materials should be addressed to D.P.B. The nine active sequences have been deposited in GenBank under accession numbers AF051883–51891.

Deep-ocean gradients in the concentration of dissolved organic carbon

Dennis A. Hansell & Craig A. Carlson

Bermuda Biological Station for Research, Inc., St Georges, GE01, Bermuda

There is as much carbon in dissolved organic material in the oceans as there is CO_2 in the atmosphere[1], but the role of dissolved organic carbon (DOC) in the global carbon cycle is poorly understood. DOC in the deep ocean has long been considered to be uniformly distributed[2,3] and hence largely refractory to biological